ISSN 1392-1207. MECHANIKA. Vol. 31, No. 2, 2025: 102–109

Dynamics of Ferromagnetic Hybrid Nanofluids in the Presence of Permeable Surface

Radha Krishnaveni TALAGADADEEVI*, Srinivasa Kumar BHAVIRISETTY, Venkata Ramana Reddy GURRAMPATI*****

**Research Scholar, Department of Mathematics, Koneru Lakshmaiah Education Foundation, Vaddeswaram, Guntur (Dt), Andhra PRADESH, India-522302. E-mail: radhaphd.18@gmail.com*

***Department of Mathematics, Koneru Lakshmaiah Education Foundation, Vaddeswaram, Guntur (Dt), Andhra PRADESH, India-522302. E-mail: sk_bhavirisetty@kluniversity.in*

****Department of Mathematics, Koneru Lakshmaiah Education Foundation, Vaddeswaram, Guntur (Dt), Andhra PRADESH, India-522302, E-mail: gvrr1976@gmail.com (Corresponding Author)*

https://doi.org/10.5755/j02.mech.38672

1. Introduction

The heat-mass transmission analysis of hybrid nanofluid (HN) has gained researchers' attention in recent times. The transport phenomenon of heat-mass transmission finds influence in numerous engineering activities such as heat transmission devices, chemical catalytic reactors, and others. Ahmad et al. [1] elucidated heat-mass transmission analysis of HN dynamics with magnetism dipole in a stretchable cylinder. Chu et al. [2] explored the heat transmission dynamics of Maxwell HNs because of the pressure gradient in rectangular regions. Ayub et al. [3] studied nanoscale heat-mass movement of magnetism 3D chemically radiative HN with magnetism in circular disks. Idowu and Falodun [4] studied the mass-heat transmission of non-Newtonian fluids through a penetrable plate by diversifying viscosity including thermal conductivity. Roy and Pop [5] studied heat-mass transmission of a hybrid name fluid dynamics with binary chemically attractive post a penetrable shrinking surface. Tassaddiq et al. [6] studied the heat-mass transmission alongside nanofluid dynamics past a circular disk. The enhancement of heat-mass transmission of MHD HN dynamics with activation energy was discussed by Shanmugapriya et al. [7]. Shoaib et al. [8] investigated the heat-mass transmission process for unsteady 3D dynamics of a HN past a stretchable region. Recently, Ferdours et al. [9] analyzed 3D BL dynamics alongside heat-mass transfer past a stagnation point flow. Sulochana et al. [10] studied Soret and chemically attractive consequences on MHD radiative dynamics past a rotating cone. Alao et al. [11] examined chemically attractive fluid over a half-infinite upright plate by considering the significance of viscous dissipative, Soret-Dufour mechanisms and thermal radiation. Daba and Devaraj [12] studied convection dynamics of unsteady hydromagnetic chemically reacting fluid past a penetrable stretching surface. Hussain et al. [13] studied MHD tangent hyperbolic dynamics past a nonlinear stretchable sheet with the significance of viscous dissipative and convective conditions. Rauf et al. [14] studied the analysis and modeling of hybrid nanofluid dynamics triggered by stationary stretched disks under the hall current effect. Raza et al. [15] explored nanolayers on biological fluids dynamics through a penetrable surface with CNT. Ali et al. [16] studied the consequence of thermal radiation together with non-uniform heat flux on MHD HN past a stretchable cylinder. Idris et al. [17] studied radiation MHD dynamics on a HN past a penetrable moving plate with joules heating and thermal ship impacts. Kodi et al. [18] studied the hall current together with the thermal radiation significance of 3D circular HN reactive dynamic past a stretchable plate. Gul et al. [19] studied the radiative dynamics of the thin film maxwell HNs on an included plate within a porous space. Zahid et al. [20] examined the coupled effect of dissipation, Lorentz force, and radiation of hybrid nanofluid dynamics past, and exponential stretchable sheet. Asjad et al. [21] studied MHD viscous nanofluid dynamics with activation energy and chemical reaction. Guedri et al. [22] studied thermal dynamics for radiative ternary HN past a nonlinear stretchable sheet based on the phenomenon of Darcy-Forchheimer. Choudhary et al. [23] Performed a study of the thermal process on two sets of ternary mixed nanoparticles based on kerosene oil. Yaseen et al. [24] elucidated heat transmission analysis of hybrid mono nanofluid dynamics between double parallel plates in a Darcy penetrable regime. Goud et al. [25] deliberates the thermal distribution of ternary HN dynamics with internal generation of heat. A theoretical study of ternary hybrid nanofluid dynamics past a non-isosolutal and non-isothermal multiple geometries has been deliberated by Ramzan et al. [26]. Rafique et al. [27] examined the mathematical inspection of MHD HN dynamics by varying viscosity as well as slip constraint past a stretchable region. Waseem et al. [28] studied entropy analysis of MHD hybrid nanoparticles with viscous dispersion. Analysis of entropy generation for MHD dynamic HN past a curve a stretching surface. Muhammed et al. [29] studied 3D MHD flour of hybrid material existing between rotating disk and heat generating. Khan et al. [30] examined MHD mixed correction HNs dynamics past a permeable moving and included flat plate. Li, S., et al [31] studied Aspects of an induced magnetic field utilization for heat and mass transfer ferromagnetic hybrid nanofluid flow driven by pollutant concentration.

This research examined the Soret-Dufour mechanisms, thermal radiation, together with heat created consequences on the ferromagnetic ($MnZnFe_2O_4$ and Fe_2O_4) type of hybrid nanofluid dynamics. Research of this nature has not been explored in literature before. This shows the uniqueness of the current research, and the following assumptions are considered to improve the novelty of this study:

- Heat and mass transfer analysis are considered on the ferromagnetic hybrid nanofluids.

- Soret-Dufour mechanisms are considered to have a significant effect on the dynamics of hybrid nanofluids; and
- An induced magnetism together with thermal process was examined on the ferromagnetic HN.

The current analysis finds applications in industrial and thermal engineering. The Soret is utilized in the separation of isotopes while thermal radiation and heat generation are employed in the thermal engineering process where the temperature is very high.

2. Mathematical Analysis

This research models the dynamics of a steady laminar alongside incompressible HN past a stretching sheet situated within a penetrable regime. An induced magnetism is significant because the Reynolds magnetic number is assumed to be higher. Hence, H_1^* represent the parallel portion while H_2^* represent the actual induced magnetism flux within the boundary layer. The level of specie concentration is inspected to be high such that the mechanisms of Soret-Dufour cannot be ignored. At the free stream, the concentration and temperature are noted to be T_∞ and C_∞. The significance of the radiative flux q_r and heat generation Q are noted to affect the hybrid nanofluid dynamics. The T_w represent wall temperature while C_w represent wall concentration. The velocity at ambient vicinity is $u_e^* = ax$ while $u_w(x) = ax$ represent wall velocity subject to a, $c \succ 0$ All fluid properties are examined to be constant while BL surmise is valid. Based on the premise stated above, the governing equations lead to:

$$\frac{\partial u_1}{\partial x}+\frac{\partial u_2}{\partial y}=0\,, \tag{1}$$

$$\frac{\partial H_1^*}{\partial x}+\frac{\partial H_2^*}{\partial y}=0\,, \tag{2}$$

$$u_1\frac{\partial u_1}{\partial x}+u_2\frac{\partial u_1}{\partial y}-\frac{\mu_e^*}{4\rho_{hnf}{}^{\pi}}\left(H_1^*\frac{\partial H_1^*}{\partial x}+H_2^*\frac{\partial H^*_1}{\partial y}\right)=$$
$$=u_e^*\frac{\partial u_e^*}{\partial x}-\frac{\mu_e^* H_e^*}{4\rho_{hnf}{}^{\pi}}\frac{\partial H_e^*}{\partial x}+\nu_{hnf}\frac{\partial^2 u_1}{\partial y^2}-\frac{\mu_{hnf}}{\kappa}u_1 \quad , \tag{3}$$

$$u_1\frac{\partial H_1^*}{\partial x}+u_2\frac{\partial H_1^*}{\partial y}=$$
$$=H_1^*\frac{\partial u_1}{\partial x}+H_2^*\frac{\partial u_1}{\partial y}+\eta_0\frac{\partial^2 H_1^*}{\partial y^2}\,, \tag{4}$$

$$u_1\frac{\partial T}{\partial x}+u_2\frac{\partial T}{\partial y}=\begin{bmatrix}\alpha_{hnf}\dfrac{\partial^2 T}{\partial y^2}+\dfrac{Q}{\rho c_p}\left(T-T_\infty\right)\\ -\dfrac{1}{\left(\rho c_p\right)_{hnf}}\dfrac{\partial q_r}{\partial y}+\dfrac{DK_T}{c_s c_p}\dfrac{\partial^2 H_1^*}{\partial y^2}\end{bmatrix} \tag{5}$$

$$u_1\frac{\partial C}{\partial x}+u_2\frac{\partial C}{\partial y}=D_m\frac{\partial^2 C}{\partial y^2}+\frac{DK_T}{T_m}\frac{\partial^2 T}{\partial y^2}\,. \tag{6}$$

Subject to the boundary conditions are:

$$u_1=u_w\left(x\right)=cx,\ u_2=0,$$
$$\frac{\partial H_1^*}{\partial y}=H_2{}^*=0,\ T=T_w,\ C=C_w : y=0\,, \tag{7}$$

$$u_1=u_e{}^*ax,\ H_1^*=H_e^*,$$
$$T=T_\infty,\ C=C_w : y\to\infty\,, \tag{8}$$

where u_1 and u_2 are velocity components, D is mass diffusivity, α means thermal diffusivity, x and y are coordinates, H_1^* and H_2^* are induced magnetism vectors, K means Boltzmann constant, $S(C)$ means external pollutant source function, β is the endothermic and exothermic factor, T and C are temperature and concentration, η_0 means magnetic diffusivity, ν means kinematic viscosity, μ_e^* is the magnetic permeability, H_e^* means ambient magnetism fields, T_∞ and C_∞ are ambient temperature together with concentration respectively. To change the modeled equations into ODEs, the following similarity variables are introduced:

$$u_1=xcf'\left(\eta\right),\ u_2=-f\left(\eta\right)\sqrt{\nu_f c},\ \eta=y\sqrt{\frac{c}{\nu_f}},$$
$$\theta=\frac{T-T_\infty}{T_w-T_\infty},\ H_1^*=H_0\left(\frac{x}{l}\right)g'(\eta),$$
$$H_2{}^*=-g\left(\eta\right)H_0\sqrt{\frac{\nu_f}{l^2 c}},\ \varphi=\frac{C-C_\infty}{C_w-C_\infty}.$$

Using the similarity transformation above to obtain the ODEs as:

$$\frac{1}{\omega_1}f'''+\omega_2\left(ff''-\left(f'\right)^2+\left(A^*\right)^2\right)+$$
$$+M\left(\left(g'\right)^2-gg''-1\right)-\frac{1}{p_0}f'=0, \tag{9}$$

$$\lambda^* g'''+g''f-gf''=0\,, \tag{10}$$

$$\frac{K}{K}\left(\frac{1+R}{pr}\right)\theta''+\omega\left(f\theta'+Q\theta+D\varphi''\right)=0\,, \tag{11}$$

$$\varphi''+Sc\left(S_0\theta''+\varphi' f\right)=0\,. \tag{12}$$

The related conditions are transformed as follows:

$$f=0,\ f'=1,\ g=0,$$
$$g''=0,\ \varphi=1,\ \theta=1,\ \eta=0\,, \tag{13}$$

$$f'=A^*,\ g'=1,\ \varphi=0,\ \theta=0,\ \eta\to 0\,, \tag{14}$$

where f, g are dimensionless stream and magnetic functions, f', g' are derivatives of dimensionless stream and magnetic functions, η is similarity variable and θ is dimensionless temperature.

3. Methodology (Spectral Relaxation Method)

This analysis uses the SRM to numerically be tackled the modified Eqs. (9)-(12) that are susceptible to (13)

and (14). SRM is a method that uses the Gauss-Seidel relaxation kind of operation to solve the structured of equations iteratively. The Gauss-Seidel relaxation method is used to both decouple and linearize the system of equations. The Chebyshev pseudo-spectral technique is used to further discretize the linearized equations. Furthermore, nonlinear terms are evaluated at the previous iteration level, but all linear terms are solved at the most recent iteration level. Using the SRM on the modified equations to produce:

$$\frac{1}{\omega_1} f'''_{r+1} + \omega_2 f_r f''_{r+1} - \omega_2 \left(f'_{r+1}\right)^2 + \omega_2 \left(A^*\right)^2 + \\ + \beta^* \left(g'_r\right)^2 - \beta^* g_r g''_r - \beta^* - \frac{1}{p_0} f'_{r+1} = 0, \quad (15)$$

$$\frac{K_{hnf}}{K_f}\left(\frac{1+R}{pr}\right)\theta''_{r+1} + \omega_3 f_{r+1}\theta'_{r+1} + \omega_3 Q_0 \theta_{r+1} + \\ + \omega_3 D_0 \varphi''_r = 0, \quad (16)$$

$$\lambda^* g'''_{r+1} + f_{r+1} g''_{r+1} - g_{r+1} f''_r = 0, \quad (17)$$

$$\varphi''_{r+1} + Scf_{r+1}\varphi'_{r+1} = 0. \quad (18)$$

The coefficient terms are explained as follows:

$$a_{0,r} = \omega_2 f_r,\ a_{1,r} = -\omega_2 \left(f'_{r+1}\right)^2,\ a_{2,r} = -\beta^* \omega_2 \left(A^*\right)^2,$$

$$a_{0,r} = \omega_2 f_r,\ a_{1,r} = -\omega_2 \left(f'_{r+1}\right)^2,\ a_{2,r} = -\beta^* \omega_2 \left(A^*\right)^2,$$

$$a_{3,r} = -\beta^* g_r g''_r,\ a_{4,r} = \beta^* \left(g'_r\right)^2,$$

$$b_{0,r} = \frac{K_{hnf}}{K_f}\left(\frac{1+R}{Pr}\right),\ b_{1,r} = \omega_3 f_{r+1}, b_{2,r} = \omega_3 Q_0,\ b_{3,r} = D_0 \varphi''',$$

$$a_{0,r} = \omega_2 f_r,\ a_{1,r} = -\omega_2 \left(f'_{r+1}\right)^2,\ a_{2,r} = -\beta^* \omega_2 \left(A^*\right)^2,$$

$$a_{3,r} = -\beta^* g_r g''_r,\ a_{4,r} = \beta^* \left(g'_r\right)^2.$$

Substituting the coefficient parameters above to obtain:

$$\frac{1}{\omega_1} f'''_{r+1} + a_{0,r} f''_{r+1} + a_{1,r} + a_{2,r} + a_{4,r} + \\ + a_{3,r} - \frac{1}{p_0} f'_{r+1} = 0, \quad (19)$$

$$b_{0,r}\theta''_{r+1} + b_{1,r}\theta'_{r+1} + b_{2,r}\theta_{r+1} + b_{3,r} = 0, \quad (20)$$

$$\lambda^* g'''_{r+1} + c_{0,r} g''_{r+1} - c_{1,r} g_{r+1} = 0, \quad (21)$$

$$\varphi''_{r+1} + d_{0,r}\varphi'_{r+1} = 0. \quad (22)$$

The equations above are discretized by employing Chebyshev spectral techniques. The discretized equations are now solved by implementing the implicit finite difference technique. Finally, the idea of SRM entails the use of differentiation matrix to simplify the unknown variable derivatives.

4. Results and Discussion

This model explained the Soret-Dufour mechanisms, induced magnetism field and radiation on the dynamics of ferromagnetic hybrid nanofluids through a stretching surface. The significant flow parameters are the Dufour term (*Do*), Soret term (*So*), thermal radiation, magnetism term (*M*), Prandtl number (*Pr*), Schmidt number (*Sc*), heat generation (Q_0), and inverse of magnetic Prandtl number. These parameters are set to be: $D_O = 2.0$, $So = 1.0$, $R = 0.5$, $M = 1.0$, $Pr = 0.71$, $Sc = 0.38$, $Q_0 = 2.0$.

All tables and graphs correspond to these values except where it is otherwise stated. The significant of the a forementioned parameters are represented on a graph to describe the problem.

Figs. 2 and 3 depicts the inspection of Soret terms S_0 on the velocity with concentration contour. Raising *So* was noticed to enhance the fluid velocity right from the wall to the free stream. On the concentration profile, increase in *So* drastically enhance the nanoparticles concentration while a decrease in the profile was observed far away from the

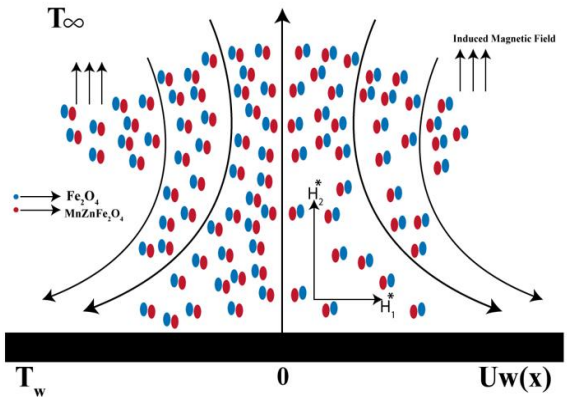

Fig. 1 Physical model of the problem

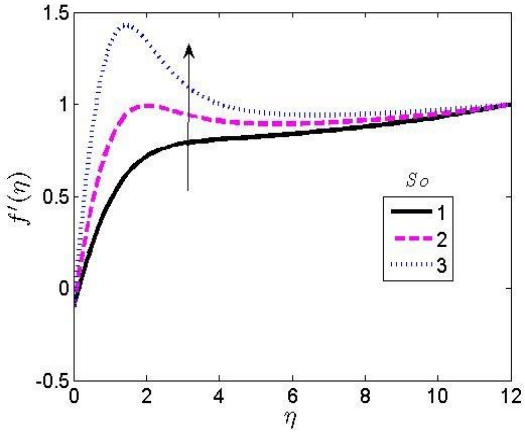

Fig. 2 Consequence of Soret number on the velocity profiles

Table 1

Thermophysical features of water, engine oil, Fe_2O_4 and $MnZnFe_2O_4$ [21]

Symbol	*Water*	*Engine Oil*	Fe_2O_4	$MnZnFe_2O_4$
ρ, kg/m^3	997.1	847.8	5181	4700
c_p, J/kgK	4179	2161	670	1050
K, W/mk	0.613	0.138	9.7	3.9
Pr	6.3	30	…	…

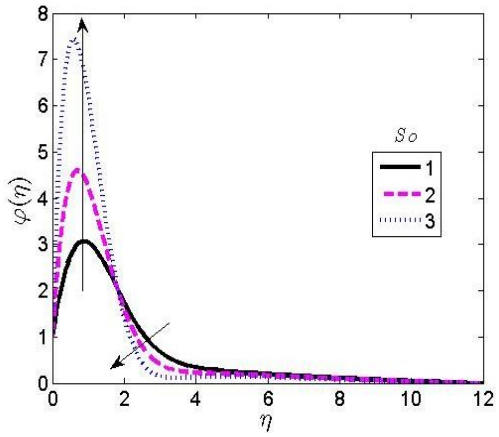

Fig. 3 Consequence of Soret number on the concentration profiles

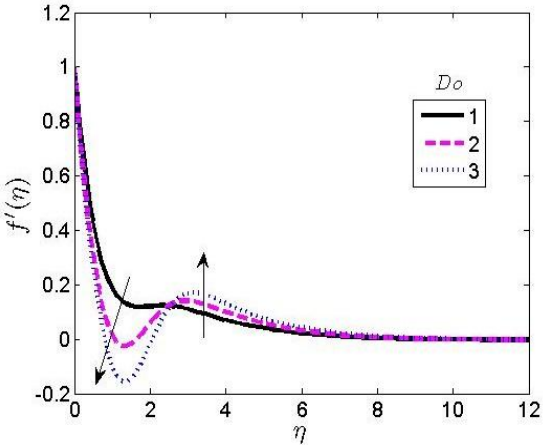

Fig. 4 Consequence of Dufour parameter on the velocity profiles

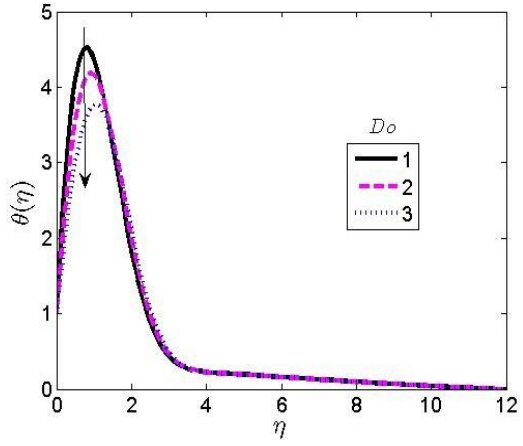

Fig. 5 Consequence of Dufour parameter on the temperature profiles

wall. In a fluid mixture, where there is a temperature gradient, the components of mixture respond differently to the gradient based on their molecular properties. The redistribution of species creates a concentration gradient driven by the thermal gradient, which is the essence of Soret effect on the flow. This is because of the magnetic forces imposed on the flow within the boundary layer. A higher magnitude of *So* enhances the heat diffusion of the fluid particles within the Boundary layer Figs. 4 and 5 are illustrates the significant impact of Dufour parameter (*Do*) on the velocity and tem-

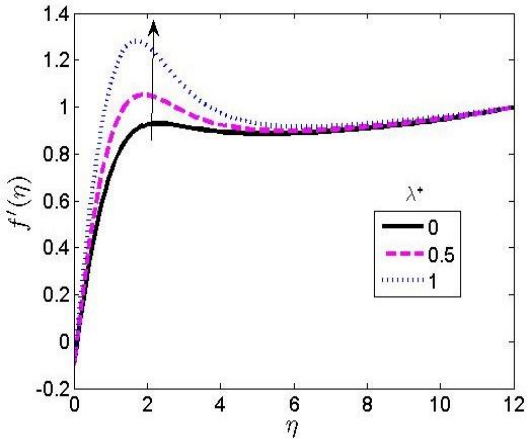

Fig. 6 Consequence of inverse magnetic Prandtl number on the velocity profiles

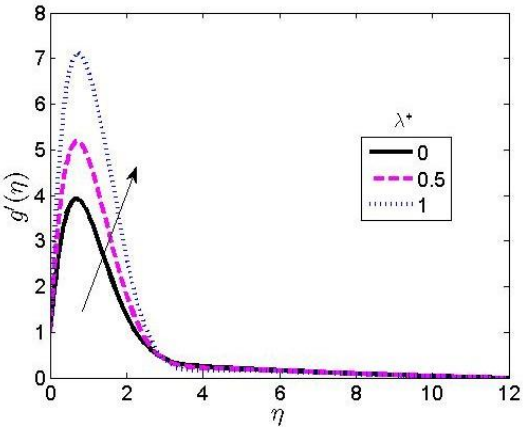

Fig. 7 Consequence of inverse magnetic Prandtl number on induced velocity profiles

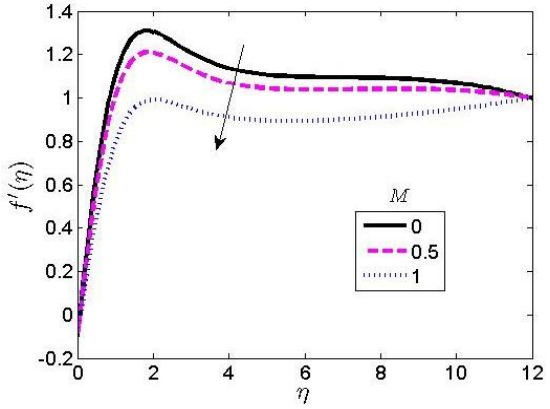

Fig. 8 Consequence of magnetic field parameter on the velocity profiles

perature contour respectively. A higher value of *Do* = 1, 2, 3shows a decrease very close to the wall while a minor increase long distance from the plate. The imposed magnetism was discovered to decrease the fluid temperature at the wall. This means that the diffusion-thermal distribution of the nanofluids cooled down due to the Lorentz force produced by magnetism. Figs. 6 and 7 depicts the inspection of inverse magnetic Prandtl λ^* on the velocity and induced velocity profile. A drastic increase in both velocity and induced velocity was due to an enlarged in λ^*. The physical behavior of the inverse magnetic Prandtl term represents the rate at which the magnetic field diffuses through the fluid

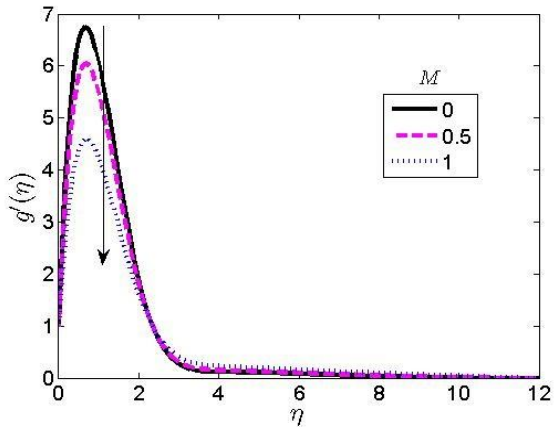

Fig. 9 Consequence of magnetic field parameter on the induced velocity profiles

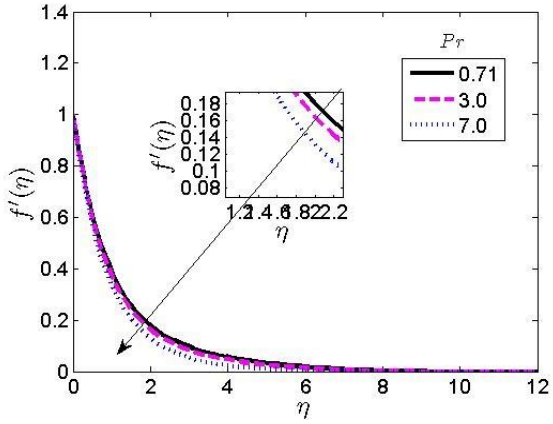

Fig. 10 Consequence of Prandtl number on the velocity with profiles

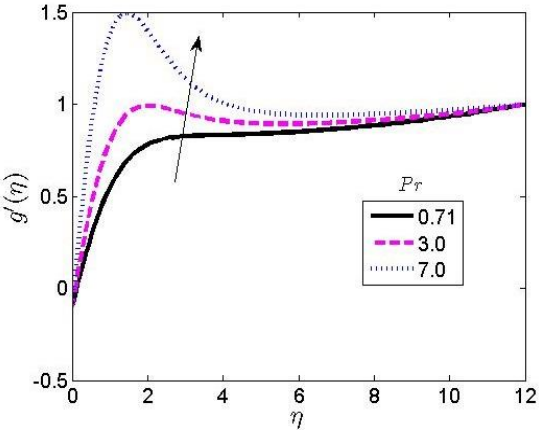

Fig. 11 Consequence of Prandtl number on the induced velocity with profiles

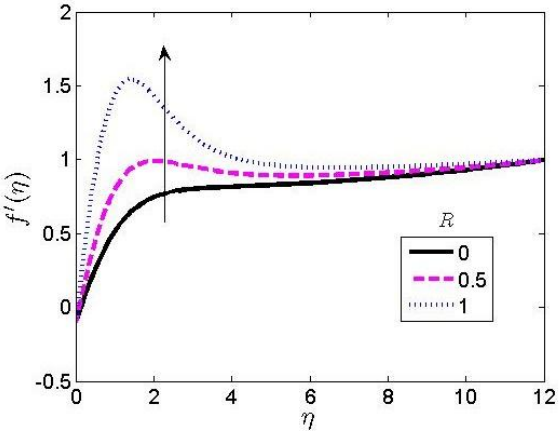

Fig. 12 Consequence of thermal radiation on the velocity contour

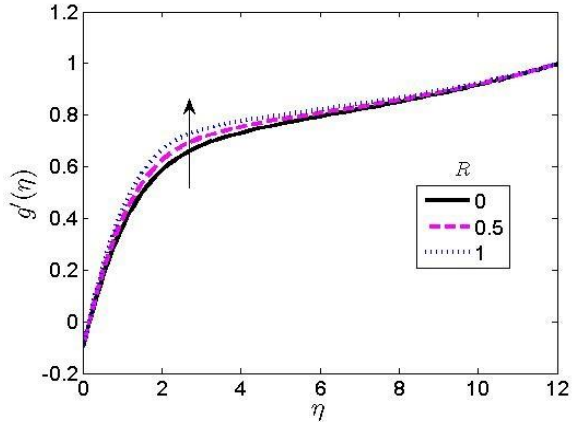

Fig. 13 Consequence of thermal radiation on temperature contour

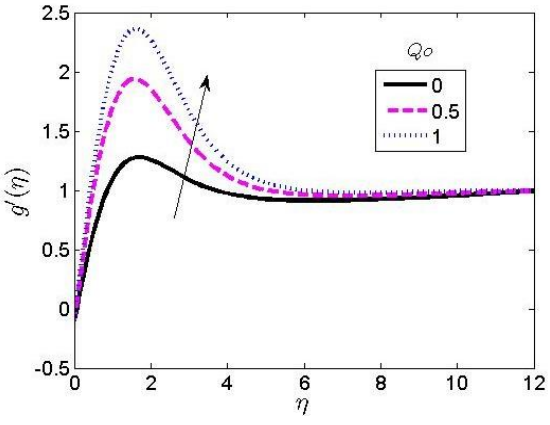

Fig. 14 Consequence of heat generation parameter on the induced velocity profiles

due to its conductivity and permeability. Physically, the induced magnetism field increases the rate of heat transmission which leads to a random collision of fluid particles. Figs. 8 and 9 are illustrating the inspection of the magnetism field (M) on f' and g' simultaneously. The magnetism field is a parameter downturn the dynamics of electrically conducting liquids due to the origination of Lorentz force. Hence, the magnetic force drags the nanofluid flow within the boundary layer. Figs. 10 and 11 displays the inspection of the Prandtl number (Pr) on the velocity and temperature contours. A decrease in the velocity profile was observed due to a higher value of Prandtl number. In addition, enlargement of Pr leads to an increase in the induced velocity. Figs. 12 and 13 inspected significant thermal radiation (R)on the velocity, induced velocity, and temperature profiles. An enlargement in the magnitude of R was detected to enlarged f', g' and θ respectively. Physically, an enlargement of R leads to an increase in fluid thermal condition. This means that thermal radiation is significant in thermal engineering whenever the temperature is high. Physically, thermal radiation helps to enhance convective flow. Hence, thermal radiation enhances the fluid thermal and momentum BL thickness. Figs. 14 and15 depict the effect of the heat generation (Qo) on the g' and θrespectively. An enlargement of Qo was

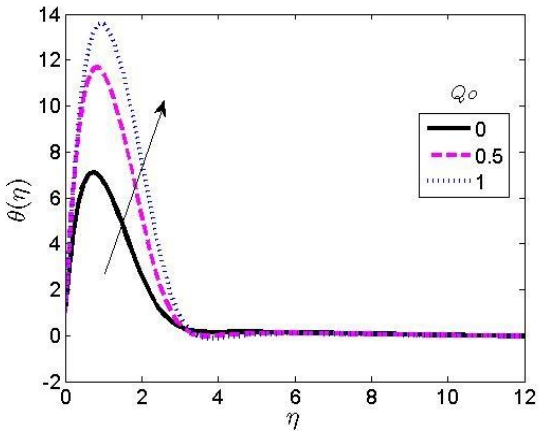

Fig. 15 Consequence of heat generation parameter on the temperature contour

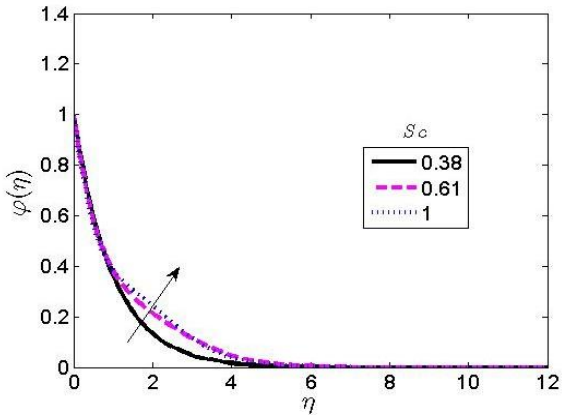

Fig. 16 Consequence of Schmidt number on the concentration profiles

detected to enhance g' and θ.This parameter generates heat within the boundary layer which enhances the fluid thermal *BL* thickness. Fig. 16 shows the impact of Schmidt (*Sc*) on the velocity with concentration contour. The examination of *Sc* is very crucial in this exploration because it explains to us the rate of mass transfer. Hence, $Sc = 0$ shows the absence of a mass transmission process. when $Sc < 1$ it means that the diffusion species is greater than the momentum diffusivity. Hence, a high *Sc* means momentum diffusion is more significant as compared to the mass flux.

5. Conclusions

In this analysis, the mechanism of Soret-Dufour, induced magnetic field and radiation significance on hybrid nanofluids has been examined numerically. The transformed model in the form of ODEs was solved by employing SRM which solves the ODEs iteratively. By virtue of the analysis in this research, we have:

1. The Soret term greatly influences the fluid concentration profile.

2. The Dufour term greatly influences the fluid temperature profile.

3. The magnetic field produces Lorentz force which drags the flow within the boundary layer by reducing the velocity profile.

4. Increase in thermal radiation enhances the fluid thermal and momentum boundary layer thickness; and

5. Increase in *Sc* depreciates the fluid velocity and concentration.

6. A robust numerical algorithm to study non-linear effects, such as chaotic flow, turbulence, or unsteady conditions in ferromagnetic hybrid nanofluids can be studied in the future.

7. Incorporate additional effects such as variable thermal conductivity, viscosity, and density stratification to make the models more realistic and applicable to a broader range of engineering problems; and

8. Investigate the potential of hybrid nanofluids in enhancing the efficiency of geothermal energy extraction or improving soil remediation techniques under controlled thermal and mass transfer conditions.

References

1. **Ahmad, F.; Abdal, S.; Ayed, H.; Hussain, S.; Salim, S.; Almatroud, A. O.** 2021. The improved thermal efficiency of Maxwell hybrid nanofluid comprising of graphene oxide plus silver/kerosene oil over stretching sheet, Case Studies in Thermal Engineering 27: 101257. https://doi.org/10.1016/j.csite.2021.101257.
2. **Chu, Y. M.; Jakeer, S.; Reddy, S. R. R.; Rupa, M. L.; Trabelsi, Y.; Khan, M. I.; Hejazi, H. A.; Makhdoum, B. M.; Eldin, S. M.** 2023. Double diffusion effect on the bio-convective magnetized flow of tangent hyperbolic liquid by a stretched nano-material with Arrhenius Catalysts, Case Studies in Thermal Engineering 44: 102838. https://doi.org/10.1016/j.csite.2023.102838.
3. **Ayub, A.; Sabir, Z.; Le, D. N.; Aly, A. A.** 2021. Nanoscale heat and mass transport of magnetized 3-D chemically radiative hybrid nanofluid with orthogonal/inclined magnetic field along rotating sheet, Case Studies in Thermal Engineering 26: 101193. https://doi.org/10.1016/j.csite.2021.101193.
4. **Idowu, A. S.; Falodun, B. O**. 2020. Variable thermal conductivity and viscosity effects on non-Newtonian fluids flow through a vertical porous plate under Soret-Dufour influence, Mathematics and Computers in Simulation 177: 358-384. https://doi.org/10.1016/j.matcom.2020.05.001.
5. **Roy, N. C.; Pop, I.** 2022. Heat and mass transfer of a hybrid nanofluid flow with binary chemical reaction over a permeable shrinking surface, Chinese Journal of Physics 76: 283-298. https://doi.org/10.1016/j.cjph.2021.10.041.
6. **Tassaddiq, A.; Khan, S.; Bilal, M.; Gul, T.; Mukhtar, S.; Shah, Z.; Bonyah, E**. 2020. Heat and mass transfer together with hybrid nanofluid flow over a rotating disk. AIP Advances 10(5): 055317. https://doi.org/10.1063/5.0010181.
7. **Shanmugapriya, M.; Sundareswaran, R.; Senthil Kumar, P.** 2021. Heat and Mass Transfer Enhancement of MHD Hybrid Nanofluid Flow in the Presence of Activation Energy, International Journal of Chemical Engineering 2021(1): 9473226. https://doi.org/10.1155/2021/9473226.
8. **Shoaib, M., Abukhaled, M.; Raja, M. A. Z.; Khan, M. A. R.; Sabir, M. T.; Nisar, K. S.; Iltaf, I.** 2022. Heat and Mass Transfer Analysis for Unsteady Three-Dimensional Flow of Hybrid Nanofluid Over a Stretching Surface Using Supervised Neural Networks, Frontiers in Physics 10: 949907. https://doi.org/10.3389/fphy.2022.949907.

9. **Ferdows, M.; Shamshuddin, M. D.; Rashad, A. M.; Murtaza, M. G.; Salawu, S. O**. 2024. Three-dimensional boundary layer flow and heat/mass transfer through stagnation point flow of hybrid nanofluid, Journal of Engineering and Applied Science 71: 57. https://doi.org/10.1186/s44147-024-00388-9.
10. **Sulochana, C.; Samrat, S. P.; Sandeep, N.** 2018. Numerical investigation of magnetohydrodynamic (MHD) radiative flow over a rotating cone in the presence of Soret and chemical reaction, Propulsion and Power Research 7(1): 91-101. https://doi.org/10.1016/j.jppr.2018.01.001.
11. **Alao, F. I.; Fagbade, A. I.; Falodun, B. O.** 2016. Effects of thermal radiation, Soret and Dufour on an unsteady heat and mass transfer flow of a chemically reacting fluid past a semi-infinite vertical plate with viscous dissipation, Journal of the Nigerian Mathematical Society 35(1): 142-158. https://doi.org/10.1016/j.jnnms.2016.01.002.
12. **Daba, M.; Devaraj, P.** 2016. Unsteady hydromagnetic chemically reacting mixed convection flow over a permeable stretching surface with slip and thermal radiation, Journal of the Nigerian Mathematical Society 35(1): 245-256. https://doi.org/10.1016/j.jnnms.2016.02.006.
13. **Hussain, A.; Malik, M. Y.; Salahuddin, T.; Rubab, A.; Khan, M.** 2017. Effects of viscous dissipation on MHD tangent hyperbolic fluid over a nonlinear stretching sheet with convective boundary conditions, Results in Physics 7: 3502-3509. https://doi.org/10.1016/j.rinp.2017.08.026.
14. **Rauf, A.; Mushtaq, A.; Shah, N. A.; Botmart, T.** 2022. Heat transfer and hybrid ferrofluid flow over a nonlinearly stretchable rotating disk under the influence of an alternating magnetic field, Scientific Reports 12(1): 17548. https://doi.org/10.1038/s41598-022-21784-2.
15. **Raza Q.; Wang, X.; Bagh, A.; Eldin S. M.; Yang, H.; Siddique, I.** 2023. Role of nanolayer on the dynamics of tri-hybrid nanofluid subject to gyrotactic microorganisms and nanoparticles morphology vis two porous disks, Case Studies in Thermal Engineering 51: 103534. https://doi.org/10.1016/j.csite.2023.103534.
16. **Ali, A.; Kanwal, T.; Awais, M.; Shah, Z.; Kumam, P.; Thounthong, P.** 2021. Impact of thermal radiation and non-uniform heat flux on MHD hybrid nanofluid along a stretching cylinder, Scientific Reports 11: 20262. https://doi.org/10.1038/s41598-021-99800-0.
17. **Idris, S.; Jamaludin, A.; Nazar, R.; Pop, I.** 2023. Radiative MHD flow of hybrid nano fluid over permeable moving plate with Joule heating and thermal slip effects, Alexandria Engineering Journal 83: 222-233. https://doi.org/10.1016/j.aej.2023.09.065.
18. **Kodi, R.; Ravuri, M. R.; Veeranna, V.; Khan, M. I.; Abdullaev, S.; Tamam, N.** 2023. Hall current and thermal radiation effects of 3D rotating hybrid nanofluid reactive flow via stretched plate with internal heat absorption, Results in Physics 53: 106915. https://doi.org/10.1016/j.rinp.2023.106915.
19. **Gul, T.; Mukhtar, S.; Alghamdi, W.; Tag Eldin, E.; Yassen, M. F.; Guedri, K.** 2022. The radiative flow of the thin-film Maxwell hybrid nanofluids on an inclined plane in a porous space, Frontiers in Energy Research 10: 970293. https://doi.org/10.3389/fenrg.2022.970293.
20. **Zahid, M.; Basit, A.; Ullah, T.; Ali, B.; Liśkiewicz, G.** 2023. Coupled Effects of Lorentz Force, Radiation, and Dissipation on the Dynamics of a Hybrid Nanofluid over an Exponential Stretching Sheet, Energies 16(21): 7452. https://doi.org/10.3390/en16217452.
21. **Asjad, M. I., Zahid, M., Jarad, F., & Alsharif, A. M.** 2022. Bioconvection flow of MHD viscous nanofluid in the presence of chemical reaction and activation energy, Mathematical Problems in Engineering 2022(1): 1707894. https://doi.org/10.1155/2022/1707894
22. **Guedri, K.; Khan, A.; Sene, N.; Raizah, Z.; Saeed, A.; Galal, A. M**. 2022. Thermal Flow for Radiative Ternary Hybrid Nanofluid over Nonlinear Stretching Sheet Subject to Darcy–Forchheimer Phenomenon, Mathematical Problems in Engineering 2022(1): 3429439. https://doi.org/10.1155/2022/3429439.
23. **Choudhary, S.; Mehta, R.; Alessa, N.; Jangid, S.; Venkateswar Reddy, M.** 2023. Thermal Analysis on Kerosene Oil-Based Two Groups of Ternary Hybrid Nanoparticles (CNT-Gr-Fe_3O_4 and MgO-Cu-Au) Mix Flow over a Bidirectional Stretching Sheet: A Comparative Approach, Journal of Engineering 2023(1): 8828300. https://doi.org/10.1155/2023/8828300.
24. **Yaseen, M., Rawat, S. K., Shafiq, A., Kumar, M., & Nonlaopon, K.** 2022. Analysis of heat transfer of mono and hybrid nanofluid flow between two parallel plates in a Darcy porous medium with thermal radiation and heat generation /absorption, Symmetry, 14(9), 1943. https://doi.org/10.3390/sym14091943
25. **Goud, J. S., Srilatha, P., Kumar, R. V., Kumar, K. T., Khan, U., Raizah, Z., ... & Galal, A. M**. 2022. Role of ternary hybrid nanofluid in the thermal distribution of a dovetail fin with the internal generation of heat. Case Studies in Thermal Engineering, 35, 102113. https://doi.org/10.1016/j.csite.2022.102113
26. **Ramzan, M., Kumam, P., Lone, S. A., Seangwattana, T., Saeed, A., & Galal, A. M.** 2023. A theoretical analysis of the ternary hybrid nanofluid flows over a non-isothermal and non-isosolutal multiple geometries, Heliyon, 9(4). https://doi.org/10.1016/j.heliyon.2023.e14875
27. **Rafique, K.; Mahmood, Z.; Khan, U.** 2023. Mathematical analysis of MHD hybrid nanofluid flow with variable viscosity and slip conditions over a stretching surface, Materials Today Communications, 36, 106692. https://doi.org/10.1016/j.mtcomm.2023.106692
28. **Waseem, F., Sohail, M., Ilyas, N., Awwad, E. M., Sharaf, M., Khan, M. J., & Tulu, A**. 2024. Entropy analysis of MHD hybrid nanoparticles with OHAM considering viscous dissipation and thermal radiation. Scientific Reports, 14(1), 1096. https://doi.org/10.1038/s41598-023-50865-z
29. **Muhammad, K.; Inayatullah; Assiri, T. A.; Shah, S. I.; Elseesy, I. E.** 2023. Three-dimensional MHD flow of hybrid material between rotating disks with heat generation, Heliyon 9(7): e18018.

https://doi.org/10.1016/j.heliyon.2023.e18018.
30. **Khan, U.; Waini, I.; Zaib, A.; Ishak, A.; Pop, I.** 2022. MHD Mixed Convection Hybrid Nanofluids Flow over a Permeable Moving Inclined Flat Plate in the Presence of Thermophoretic and Radiative Heat Flux Effects, Mathematics 10(7): 1164. https://doi.org/10.3390/math10071164.
31. **Li, S.; Saadeh, R.; Madhukesh, J. K.; Khan, U.; Ramesh, G. K.; Zaib, A.; Prasannakumara, B. C.; Kumar, R.; Ishak, A.; Sherif, E. S. M.** 2024. Aspects of an induced magnetic field utilization for heat and mass transfer ferromagnetic hybrid nanofluid flow driven by pollutant concentration, Case Studies in Thermal Engineering 53: 103892. https://doi.org/10.1016/j.csite.2023.103892.

R. K. Talagadadeevi, S. K. Bhavirisetty,
V. R. R. Gurrampati

DYNAMICS OF FERROMAGNETIC HYBRID NANOFLUIDS IN THE PRESENCE OF PERMEABLE SURFACE

S u m m a r y

This research examined the dynamics of ferromagnetic hybrid nanofluid with the consequences of heat generation, thermal radiation, and Soret-Dufour mechanisms. The thermal procedure was inspected with induced magnetism and permeable stretching surface. The physical model interpretation is represented by partial differential equations (PDEs). By implementing a suitable transformation function, the set of PDEs is changed into ordinary differential equations (ODEs). The spectral relaxation technique (SRM) is further implemented to solve the set of ODEs. The SRM was implemented to iteratively solve the equations of ODEs by considering the linear terms and nonlinear terms at current and previous iterations. Thermal analysis greatly enhances the thermal condition and the opacity of the thermal boundary layer (BL). Dufour enhances the temperature contour while the Soret enhances the concentration contour. The current outcome as compared with previous work is discovered to be in good agreement.

Key words: ferromagnetic, hybrid nanofluid, heat generation, thermal radiation, Soret-Dufour effects, induced magnetism.

Received September 1, 2024
Accepted August 22, 2025